

Hybrid Aerial and Scansorial Robotics

Alexis Lussier Desbiens, Alan Asbeck, and Mark Cutkosky

Abstract— We present an approach that builds upon previous developments in unmanned air vehicles and climbing robots and seeks to emulate the capabilities of bats, insects and certain birds that combine powered flight with the ability to land and perch on sloped and vertical surfaces. As it approaches a wall, the plane executes an intentional pitch-up maneuver to shed speed and present its feet for landing. On contact, a nonlinear suspension dissipates the remaining kinetic energy and directs interaction forces toward the feet to engage small asperities on surfaces such as brick or concrete. The focus of the work in this paper is on the controller used for sensing a wall and executing vertical landing and take-off procedures and on the mechanisms developed for spine engagement and disengagement.

I. INTRODUCTION

In comparison to other small robots, unmanned air vehicles have the ability to travel very rapidly to remote locations, including sites such as the tops of buildings or bridges that are hard to reach with terrestrial robots. However, they are subject to a severe tradeoff between payload and mission life. In contrast, climbing robots can remain perched at remote sites for hours or days, providing a secure, stable platform for inspection or surveillance. The work described in this paper is aimed at combining the best attributes of aerial and vertical surface (scansorial) robots. We focus on landing and perching on vertical surfaces for a couple of reasons. Vertical surface landing allows us to use gravity to slow the plane and engage gripping mechanisms. Also, vertical surfaces tend to be relatively safe, unobtrusive and uncluttered locations for sheltering a small, fragile vehicle – particularly if it can take shelter under the eaves of a building.

Our work builds upon developments in acrobatic maneuvers for small unmanned air vehicles and on climbing robots that attach to vertical surfaces using arrays of miniature spines. In other recent publications we describe the dynamic model of the plane and its highly damped, nonlinear suspension that dissipates kinetic energy on landing and directs interaction forces toward the spines to engage them [1], [2]. In this paper we focus on a new controller used for powered landings and takeoffs from vertical surfaces and on a new spine engagement and disengagement mechanism needed for reliably taking off from the wall. We demonstrate the overall approach used for scansorial landing, perching and take-off, and conclude with a discussion of future work needed to improve the robustness of the system with respect to disturbances (e.g. wind gusts). Future developments will

address landing on sloped and horizontal surfaces and on mechanisms for crawling along the surface after landing.

II. PREVIOUS WORK

The work described in this paper draws upon previous work on small aerial platforms that execute maneuvers suitable for landing and perching, climbing robots, and biological studies of creatures that combine aerial and scansorial capabilities.

A. Perching and takeoff maneuvers

Several researchers have demonstrated approaches by which a small plane can execute the maneuvers needed to land and perch on a target such as a branch or pole. Some of the initial work in this field includes [3] on indoor hovering and level flight and how to transition back and forth between these states as well as methods for autonomous landing and takeoff from a specially designed stand. An accurate motion capture system was used to estimate the states of the airplane and control was done using an off-board computer. Recent work [4] has used a similar motion capture system to learn a highly accurate model of the aerodynamics of a small glider. This model was used to demonstrate perching on a wire using a pitch-up maneuver to slow the airplane before contact. Further work has demonstrated [5] that, at least for a glider, there is a lack of controllability at very low speeds. A different approach involving a plane with morphing geometry [6] provides more control at low speeds. A variation on this approach is undergoing wind tunnel testing [7].

Much of the initial work on developing controllers and trajectories for dynamic perching has taken advantage of off-board motion capture and control systems. However, the capabilities of lightweight onboard sensing and control systems are also improving. Work on autonomous hovering [8] made use of a 30g Microstrain IMU (3-axis attitude sensor) to control the attitude of the plane and transition between regular flying and hovering. Other lightweight sensors [9] and autopilot boards, like the Paparazzi open-source autopilot [10], are becoming available, providing a basis autonomous perching and takeoff.

B. Climbing robots

From the literature on climbing robots, light weight and low-power technologies for climbing vertical surfaces are particularly relevant. The work described here utilizes the microspine technology developed for Spinybot [11] and RISE [12] to climb a variety of vertical surfaces including concrete, stucco and brick. The miniature spines perch on asperities (small bumps and pits) on the surface and a compliant

Alexis Lussier Desbiens and Alan Asbeck are Ph.D. Candidates in Mechanical Engineering and Electrical Engineering at Stanford University, Stanford, USA {alexisl, aasbeck}@stanford.edu

Mark Cutkosky is Professor of Mechanical Engineering at Stanford University, Stanford, USA cutkosky@stanford.edu



Fig. 1. Sequence of the plane performing a powered perching maneuver on a concrete wall. The plane is initially flying around 10 m/s, detects the wall at 6m and initiates a pitch up. The motor is turned off as soon as touchdown is possible, and the plane generally contacts the wall while moving at 0-2.7m/s in the horizontal direction. The landing gear finally absorbs the impact and engages the spines. The entire process takes < 1 sec.

suspension promotes spine engagement and ensures that the overall load is distributed among the spines. The spines have the advantages that they are lightweight, passive, and relatively unaffected by dirty or dusty surfaces. They can be used for thousands of attachment/detachment cycles and do not leave any trace of their passage.

C. Hybrid platforms

Relatively few hybrid aerial/terrestrial platforms have been demonstrated. However, one early example is a flying/walking platform [13] that combines a small flexible wing MAV with the Whegs technology from CWRU. Although not able to perch, it can land on horizontal surfaces, fold its wings and crawl. The USAF Academy has also investigated innovative concepts for flying and perching [14]. Their most successful concept was a plane equipped with a sticky pad at the nose. After flying into a wall, the plane hangs from the sticky pad by a tether, which can be cut to resume flight. Our own approach began with an investigation of strategies for landing and attaching to vertical walls using spines. In previous papers [1], [2] we present the dynamic model of the airplane with its highly compliant and damped landing gear that prevents it from bouncing off the wall and promotes attachment of microspines.

D. Aerial/Scansorial Biological Systems

Many animals including birds, insects, bats, and flying squirrels and lizards have the ability to fly or glide to a destination and perch. However, there is comparatively little work on the details of landing and take-off. The flying squirrel can land on vertical tree trunks using a maneuver somewhat like that of our plane. Its stretched skin flaps provide a low aspect ratio wing that provides aerodynamic stability and lift at angles of attack up to 40 degrees. It has been shown that the squirrels deliberately stall themselves prior to impact, allowing them to reduce by 60% their horizontal velocity, while spreading the impact over all four limbs [15], [16]. As for takeoff, it has been shown that pigeons generate up to 2.3g of acceleration with their legs prior to the start of flapping flight [17]. This initial jump allows them to increase their initial speed and clear obstacles for their wings. At a

much smaller scale, flies make dramatic use of their legs for becoming airborne, using different strategies for voluntary and emergency takeoffs [18].

III. SYSTEM OVERVIEW

Our approach uses an aerobatic plane to fly toward the wall, intentionally pitch up just before impact to slow down, and dissipate the remaining kinetic energy with a suspension that keeps forces on the microspine toes within a safe region, as shown in figure 1. The details of the perching strategy implemented on a glider can be found in [1]. This landing method allows the plane to approach the wall at its normal flying speed. Once the plane has pitched up, it is essentially ballistic. The entire maneuver requires < 0.75s, which minimizes the effects of disturbances.

The airframe that we are using (fig. 2 left) is a modified Flatana airplane, with a brushless motor and 9x3.8 APC propeller, to which we added a Paparazzi autopilot [10], 3-axis accelerometer (ADXL335), 3-axis gyroscope (IDG500) and ultrasound sensor (Maxbotix MB1320) for wall detection.

We developed a highly compliant and damped suspension (fig. 2 center) to permit a relatively large envelope of initial contact conditions: 0-2.7 m/s forward velocity, up to 3 m/s downward velocity, and pitch angles from 50-110 deg. [2]. The suspension has effectively three joints with bending at the hip and knee and stretching at the spines. Each foot has five spines to share the load over several asperities.

The aircraft re-launches from a perched position into normal flight. It uses a spine-release mechanism to disengage the spines; then the thrust from the propeller moves the plane away from the wall backwards, in a manner similar to hovering flight.

IV. POWERED PERCHING

A multiple-exposure photograph illustrating the perching sequence is shown in figure 1. In this figure, the plane is initially flying around 10 m/s; it detects the wall at 6m and commands a full up elevator to initiate the pitch up maneuver. As the pitch angle approaches 75 deg, the motor is turned off and the rotation of the airplane slowed down by the elevator. As the pitch approaches 90 deg, the plane's flight

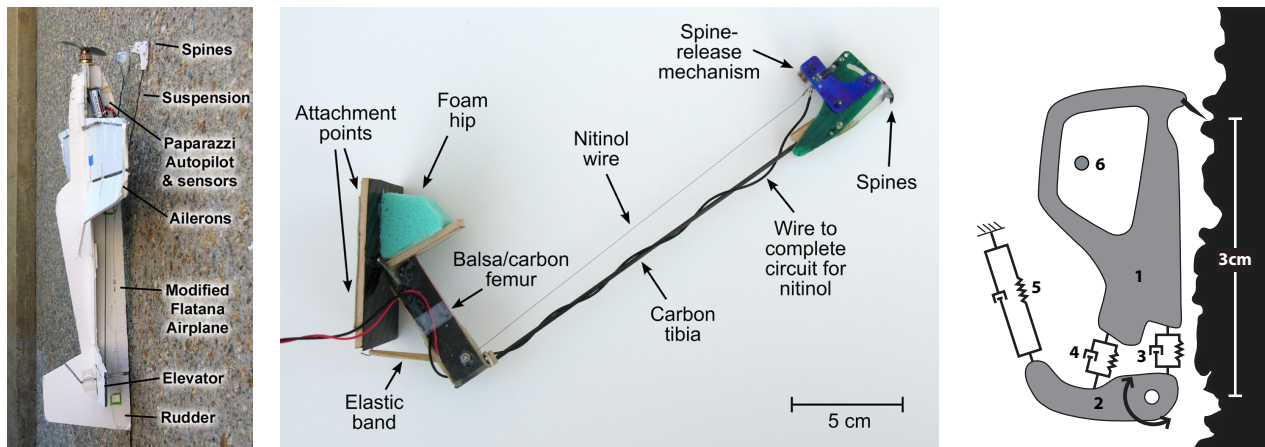


Fig. 2. Left, picture of the plane equipped with sensors and perching landing gear. Center, suspension to absorb energy while landing, including spine-release mechanism. Right, diagram of spine linkage. The spine is embedded in element 1, and can move compliantly due to flexures 3, 4, and 5. The linkage pivots around the hole in element 2.

is essentially ballistic and the plane contacts the wall while moving at roughly 2.5 m/s in the horizontal direction and 2m/s in the downward direction. At impact, the landing gear absorbs the remaining kinetic energy and engages the spines.

The strategy for powered perching is similar to that used for gliding perching in [1], but the addition of a motor and propeller presents additional benefits and challenges. The motor allows the plane to fly more slowly and at higher pitch angles, if desired, as it approaches the wall. During the pitch-up maneuver, thrust from the propeller can be used to extend the region in which the plane is ready to contact the wall. However, with the propeller in the front of the aircraft, power must be cut before the plane hits the wall. In our implementation, the propeller is de-powered as the aircraft reaches a pitch angle of 75 deg., providing some thrust through the pitch-up phase and allowing the propeller to passively slow down and stop rotating before wall contact. If the propeller is stopped suddenly, the change in angular momentum will cause the aircraft to roll (in level flight) and then yaw as the plane pitches up. We stop the propeller early and slowly during the maneuver, while the velocity of the plane is still high, so that the control surfaces can compensate for the change in angular momentum.

A powerful ultrasonic sensor (Maxbotix MB1320) is now used, as the LV-EZ2 was sensitive to the acoustical noise created by the propeller. Unfortunately, the new sensor has an update rate of only 10 Hz, which prevents us from obtaining multiple measurements of the wall position before triggering the maneuver. Multiple measurements would be useful as the plane could confirm the wall's presence and compute the approach velocity. Currently, we assume the approach velocity is around 10m/s, and, after our first detection of the wall, trigger the maneuver after an appropriate delay. Ultimately, an optical or vision-based sensor may be more useful in providing good velocity information.

Figure 3 shows the plane's velocity during a landing maneuver performed in the air, to observe the trajectory without the influence of the wall. After the plane pitches

up, gravity acts quickly in the y -direction, decreasing the velocity. The plane is only able to land if the x - and y -velocities are both within acceptable ranges, which only occurs for a short period of time (around 0.15 sec). This short time corresponds to a need to sense the distance to the wall with an accuracy of ± 20 cm.

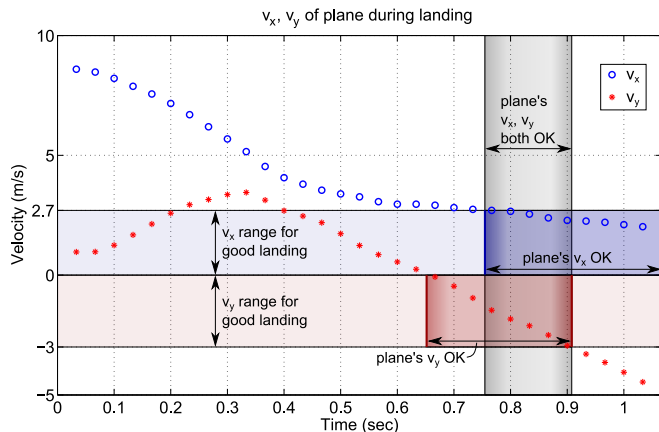


Fig. 3. Plot of plane's x - and y -velocities during a landing maneuver performed in the air. The plane is within the envelope of possible v_x and v_y for landing during only a short time. Data plotted was extracted from a video of the plane at 30 frames/sec.

V. TAKEOFF

Various strategies can be used to take off from vertical surfaces depending on the airframe configuration, its orientation on the wall and the complexity of the takeoff mechanism. For example, an airplane with a low thrust-to-weight (T/W) ratio would probably benefit from a jumping mechanism (as in [19]) to increase its initial speed and reorient itself for flight. Although we are ultimately interested in low T/W airframes for efficiency reasons, we describe here an approach used with an acrobatic platform with $T/W > 1$. Such a platform has the possibility to hover briefly, building horizontal velocity before resuming normal flight. Although

less efficient, this strategy allows for a smooth and controlled takeoff and prevents any loss of elevation in tight spaces. We anticipate that future work with low T/W planes will be able to incorporate some of the same components and methods that we describe here.

Our approach consists of releasing the spines using a specially designed mechanism and starting the takeoff once free from the wall. Then, using the high T/W ratio and propwash over its control surfaces, the airplane holds its nose up and away from the wall to build horizontal speed before resuming flight.

The use of microspines with a compliant suspension has the advantage of not requiring any special fixtures to land on, but also produces some challenges during takeoff. Although the spines will tend to disengage when the tangential load (due to gravity) is removed, the suspension is sufficiently compliant that a large excursion is required to unload the spines. If the propeller is used to generate upward thrust, the spines tend to act as a pivot, around which the plane rotates until the propeller hits the wall. Furthermore, any differences in the timing of release of the spines will cause the plane to yaw and possibly roll as the propeller pulls the plane away from the wall. For these reasons, it was decided to add an active mechanism to retract the spines on command.

A. Spine release mechanism

To release the spines, a nitinol wire pulls on an arm that lifts the spines away from the wall. The spines are embedded in elastic linkages (shown schematically in fig. 2) that are supported in front by a pin connected to a release arm (elements 6 and 4, respectively, in fig. 4). As the wire contracts, the arm rotates backward about pin 3, detaching the spines from the wall. As they disengage, the spine linkages rotate backward about pin 2 in figure 4, producing a motion that will prevent the spines from jamming in deep holes or cracks on the surface.

On each leg, a $150\mu\text{m}$ diameter, 18.5cm long strand of Flexinol brand nitinol wire is driven with 1.25 Amps. This causes the wire to contract 0.6cm in <0.15 seconds. The current is held on for slightly longer to ensure the spines have fully released. When the current is stopped, the nitinol requires a force of 0.62N to re-extend, and this is provided by a spring, element 7 in fig. 4.

B. Attitude Estimation and Control

Attitude estimation is particularly important during an almost-hovering takeoff as there are multiple sources of disturbances causing roll and yaw error, such as timing delays in the feet releasing, torque from the propeller inertia, and drag. Furthermore, it is important to control the pitch angle, so that the plane flies away from the wall and resumes normal flying.

The attitude during takeoff is obtained by integrating the gyroscope information. Because the plane is stationary before takeoff, the accelerometer can be used to measure the starting pitch and yaw attitude, providing the integration with accurate initial conditions. Our implementation further

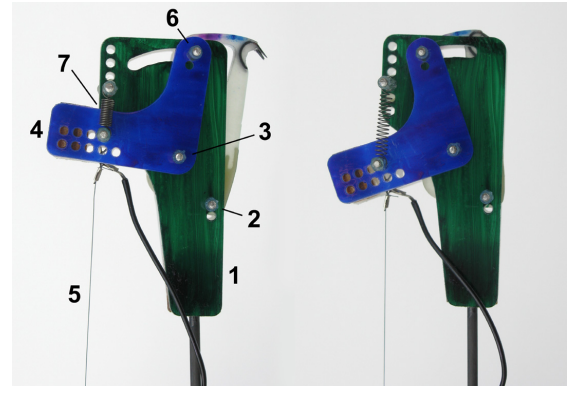


Fig. 4. Foot and mechanism to release spines. Two side plates, element 1, hold 5 spines and their linkages between them via pins (elements 2, 3). The spine linkages rotate around pin 2, and are prevented from rotating clockwise by pin 6, which is held by element 4, the release arm. When a nitinol wire, element 5, contracts, the release arm rotates backward around pin 3, lifting the fronts of the spines with pin 3. A spring, element 7, stretches the nitinol wire after disengagement and returns the release arm to its original position. Right image shows configuration with spines retracted.

assumes the initial roll angle to be 0 degrees (on the wall). After these initial conditions are set, the attitude is estimated from integration of the gyroscope angular rate to euler parameters:

$$\begin{bmatrix} \dot{\epsilon}_0 \\ \dot{\epsilon}_1 \\ \dot{\epsilon}_2 \\ \dot{\epsilon}_3 \end{bmatrix}_m = \frac{1}{2} \begin{bmatrix} -\epsilon_1 & -\epsilon_2 & -\epsilon_3 \\ \epsilon_0 & -\epsilon_3 & \epsilon_2 \\ \epsilon_3 & \epsilon_0 & -\epsilon_1 \\ -\epsilon_2 & \epsilon_1 & \epsilon_0 \end{bmatrix}_m \begin{bmatrix} w_x \\ w_y \\ w_z \end{bmatrix} \quad (1)$$

where the euler parameters are defined has $\epsilon_0 = \cos(\alpha/2)$ and $\epsilon_i = \sin(\alpha/2)\vec{\lambda} \cdot \vec{b}_i$ for a rotation of α around the unit vector $\vec{\lambda}$.

Equation 1 is then integrated at 60 Hz using trapezoidal integration to obtain the attitude, q_m , in euler parameters. With calibration of the gyroscope bias before takeoff, the attitude drift during a 30 second period is less than 1 degree, more than adequate to complete the maneuver and resume normal flight.

During takeoff, the plane's desired attitude is set to roll, pitch and yaw of $[0, 120, 0]$ degrees ($q_d = [0.5, 0, \sqrt{3}/2, 0]^T$). A pitch angle of 120 degrees allows the plane to move away from the wall and maintain its altitude while increasing the forward velocity to resume normal flight. The attitude error is then defined as the difference between the desired and current attitude, expressed as:

$$q_m = q_e \otimes q_d \quad (2)$$

where \otimes represents the quaternion product and q_e the attitude error in euler parameters. Using the preceding equation, the attitude error can be calculated with:

$$q_e = \begin{bmatrix} \epsilon_0 & -\epsilon_1 & -\epsilon_2 & -\epsilon_3 \\ \epsilon_1 & \epsilon_0 & -\epsilon_3 & \epsilon_2 \\ \epsilon_2 & \epsilon_3 & \epsilon_0 & -\epsilon_1 \\ \epsilon_3 & -\epsilon_2 & \epsilon_1 & \epsilon_0 \end{bmatrix}_m \begin{bmatrix} \epsilon_0 \\ -\epsilon_1 \\ -\epsilon_2 \\ -\epsilon_3 \end{bmatrix}_d \quad (3)$$



Fig. 5. A multiple-exposure photograph of the takeoff sequence. The airplane is originally at rest on the wall with ailerons and elevator ready for takeoff. The propeller is then commanded to a T/W ratio slightly less than 1.0; spines are released and the T/W ratio is increased to about 1.08 as the pitch angle is controlled to approximately 120 degrees from horizontal. Note that the spines have been intentionally released early in this example to clearly illustrate this step, but with ideal timing no vertical drop is observed.

The attitude error in euler parameters (q_e) can then be converted to roll, pitch and yaw errors. Care must be taken during this last conversion as it is singular for a pitch error of ± 90 degrees. Fortunately, with a good controller and careful setting of the desired attitude, this situation can be avoided. The roll, pitch and yaw errors are then controlled using the aileron, elevator and rudder. Three lead controllers are used, which have the form:

$$K_i(s) = k_i \times \frac{s + 5.3}{s + 26.5} \quad (4)$$

where the gain k_i is adjusted for each controller.

C. Control Sequence

The control sequence is illustrated in figure 6. The sequence starts by estimating the attitude using gravity measurement from the accelerometer, and resetting the gyro bias. After this initialization step, the ailerons are commanded to ± 30 degrees of trim, the attitude control is enabled and the propeller is slowly ramped up to a thrust to weight (T/W) ratio slightly below 1.0. This prevents the plane from falling too quickly when the spines are released.

When ready for takeoff, the spines are released. The nitinol wire mechanism retracts the spines in about 150 milliseconds and the T/W ratio can be increased soon after. It is generally desirable to increase the T/W ratio as soon as the spines are released to help the spines in their disengaging motion and prevent any vertical drop and downward velocity. However, we have also experimented with a maximum delay of 250 milliseconds, which causes the plane to drag its feet for about 20 cm on the wall before taking off.

The nitinol wire mechanism is turned off 50 milliseconds after increasing in T/W ratio, but the spines are not ready for any new engagements for another 0.5 seconds due to the slow cooling and relaxation of the nitinol. This delay helps

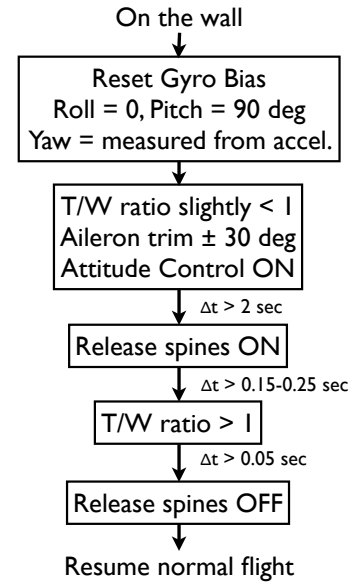


Fig. 6. Control sequence and timing during takeoff. The spines can be released between 0.15 and 0.25 seconds to control how much vertical height is lost during the maneuver.

to ensure that the plane is sufficiently away from the wall that the spines cannot inadvertently catch again.

D. Results

Numerous takeoffs have been performed using the spine release mechanism and controller described in the previous sections. A typical takeoff sequence is illustrated in fig. 5. In this case, the takeoff was delayed for an extra 250 milliseconds after the spines were released. With a shorter delay, it is possible to take off without any loss in elevation. On the accompanying video, it is possible to observe the plane dropping about 20 cm before the T/W ratio becomes

sufficient to propel the plane upward. One can also observe that the right leg is released slightly before the left one, causing an initial roll disturbance that is compensated for during the maneuver. Overall, the maneuver illustrated in fig. 5 lasts about 2 seconds, after which it is possible to do a 180-degree roll and resume normal flight.

VI. CONCLUSIONS AND FUTURE WORK

Autonomous landing and perching followed by takeoff have been demonstrated on vertical surfaces. The approach is particularly useful for landing on locations where horizontal surfaces may be cluttered and where a runway for landing and takeoff is not available. Due in part to the use of a highly compliant landing gear, an active spine release mechanism is needed to achieve reliable disengagement prior to takeoff.

Unlike on landing, on takeoff it is difficult to avoid a period of low-speed flight. (Even with a jump-assisted takeoff, a plane may need some time to achieve full airspeed.) During this time, it is important to have accurate roll, pitch and yaw controllers to compensate for disturbances. Because the plane starts from a known stationary orientation, it suffices to integrate gyroscope information to estimate the attitude during the ≈ 2 second maneuver.

Although a high thrust/weight ratio plane is less efficient than conventional aircraft, it provides benefits in terms of controllability in tight spaces during takeoff. Given that the plane only requires a straight line-of-sight approach to be able to land on a surface, it is ideal if the space required for takeoff is no larger. The high thrust/weight ratio also provides for a fail-safe approach on landing; if the spines fail to engage, the plane can immediately switch to the takeoff procedure and fly away from the wall for another attempt. Typically, however, the plane will grasp surfaces almost immediately on landing. Therefore, sliding along the surface during a failed landing should be easy to detect before the plane gathers too much downward velocity. Takeoff after a short downward fall following spine release has already been demonstrated, so this maneuver can be included directly.

Looking ahead, a number of additional developments are needed to provide a reliable hybrid aerial/scansorial platform. The ultrasonic sensor should be replaced or augmented with optical sensing for greater reliability and the aircraft controller should be enhanced for more robust flying in ambient conditions. We are also interested in being able to crawl and maneuver to reorient the plane on the wall after landing. This capability will require the use of opposed pairs of spines that can grip when loaded in any direction (the current spines grip only when the plane is oriented nose-upward) and a more efficient spine disengagement mechanism that can be applied with every step.

VII. ACKNOWLEDGMENTS

Alexis Lussier Desbiens is supported by the Natural Sciences and Engineering Research Council of Canada and the Organization of American States, with additional support from DARPA DSO. We would also like to thank the members of BDML at Stanford for all their help in conducting the

experiments reported here. Many thanks to Dharma Tamm, Matthew Norcia and Kwame Agyei-Owusu for building so many prototypes over the summer.

REFERENCES

- [1] A. Lussier Desbiens and M. Cutkosky, "Landing and Perching on Vertical Surfaces with Microspines for Small Unmanned Air Vehicles," *2nd International Symposium on Unmanned Aerial Vehicles*, 2009.
- [2] A. Lussier Desbiens, A. Asbeck, and M. Cutkosky, "Scansorial Landing and Perching," *14th International Symposium on Robotics Research*, 2009.
- [3] A. Frank, J. S. McGrew, M. Valenti, D. Levine, and J. P. How, "Hover, transition, and level flight control design for a single-propeller indoor airplane," *AIAA Guidance, Navigation and Control Conference*, Aug 2007.
- [4] R. Cory and R. Tedrake, "Experiments in fixed-wing uav perching," *Proceedings of the AIAA Guidance, Navigation, and Control Conference*, Aug 2008.
- [5] J. Roberts, R. Cory, and R. Tedrake, "On the controllability of fixed-wing perching," *American Controls Conference*, Sep 2009.
- [6] A. Wickenheiser and E. Garcia, "Perching aerodynamics and trajectory optimization," *Proceedings of SPIE*, Jan 2007.
- [7] G. Reich, M. Wojnar, and R. Albertani, "Aerodynamic Performance of a Notional Perching MAV Design," *47 th AIAA Aerospace Sciences Meeting*, 2009.
- [8] W. Green and P. Oh, "Autonomous hovering of a fixed-wing micro air vehicle," *IEEE International Conference of Robotics and Automation*, 2008.
- [9] A. Baerveldt and R. Klank, "A low-cost and low-weight attitude estimation system for an autonomous helicopter," in *1997 IEEE International Conference on Intelligent Engineering Systems*. Institute of Electrical & Electronics Engineers (IEEE), 1997, p. 391.
- [10] Paparazzi, "Paparazzi, the free autopilot," 2008. [Online]. Available: <http://paparazzi.enac.fr>
- [11] A. Asbeck, S. Kim, M. Cutkosky, W. R. Provancher, and M. Lanzetta, "Scaling hard vertical surfaces with compliant microspine arrays," *International Journal of Robotics Research*, vol. 25, no. 12, p. 14, Sep 2006.
- [12] M. Spenko, G. Haynes, J. Saunders, M. Cutkosky, A. Rizzi, and R. Full, "Biologically inspired climbing with a hexapedal robot," *Journal of Field Robotics*, Feb 2008.
- [13] R. J. Bachmann, F. J. Boria, P. G. Ifju, R. D. Quinn, J. E. Kline, and R. Vaidyanathan, "Utility of a sensor platform capable of aerial and terrestrial locomotion," *International Conference on Advanced Intelligent Mechatronics*, pp. 1581–1586, Aug 2005.
- [14] M. Anderson, C. Perry, B. Hua, D. Olsen, J. Parcus, K. Pederson, and D. Jensen, "The Sticky-Pad Plane and other Innovative Concepts for Perching UAVs," *47 th AIAA Aerospace Sciences Meeting*, 2009.
- [15] G. Byrnes, N. T.-L. Lim, and A. J. Spence, "Take-off and landing kinetics of a free-ranging gliding mammal, the malayan colugo (*Galeopterus variegatus*)," *Proceedings of the Royal Society B: Biological Sciences*, vol. 275, no. 1638, pp. 1007–1013, Feb 2008.
- [16] K. E. Paskins, A. Bowyer, W. M. Megill, and J. S. Scheibe, "Take-off and landing forces and the evolution of controlled gliding in northern flying squirrels *glaucomys sabrinus*," *Journal of Experimental Biology*, vol. 210, no. 8, pp. 1413–1423, Apr 2007.
- [17] F. H. Heppner and J. G. Anderson, "Leg thrust important in flight take-off in the pigeon," *Journal of Experimental Biology*, vol. 114, pp. 285–288, Mar 1985.
- [18] G. Card and M. Dickinson, "Performance trade-offs in the flight initiation of *Drosophila*," *Journal of Experimental Biology*, vol. 211, no. 3, p. 341, 2008.
- [19] M. Kovac, M. Fuchs, A. Guignard, J.-C. Zufferey, and D. Floreano, "A miniature 7g jumping robot," *International Conference on Robotics and Automation*, pp. 373–378, 2008. [Online]. Available: http://ieeexplore.ieee.org/xpls/abs_all.jsp?arnumber=4543236